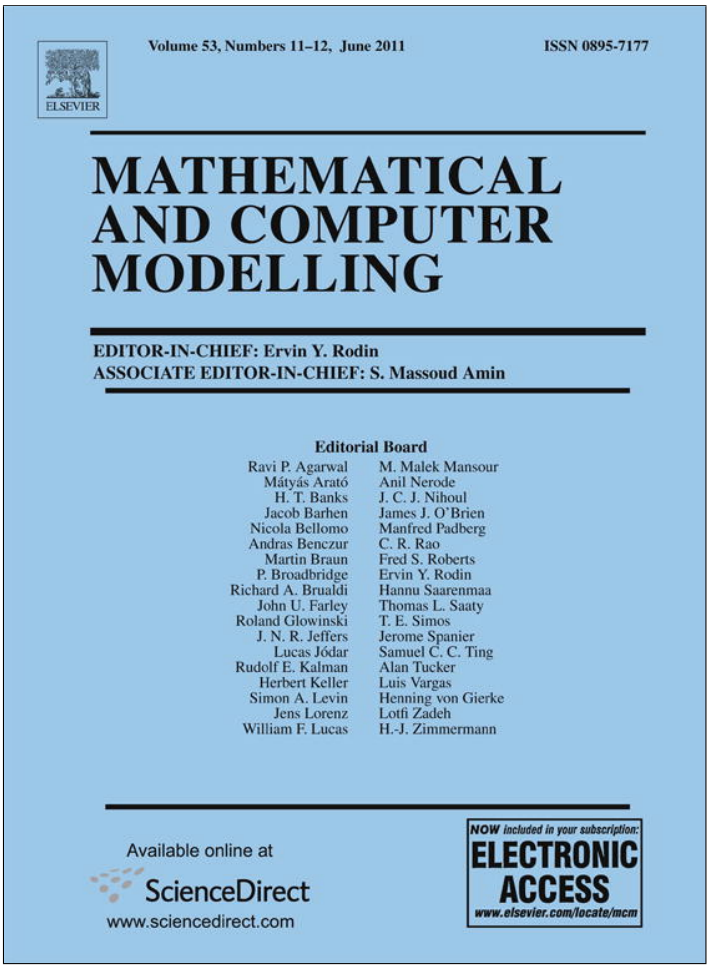

Mathematical and Computer Modelling 53 (2011) 2119–2135

Contents lists available at ScienceDirect

Mathematical and Computer Modelling

journal homepage: www.elsevier.com/locate/mcm

Mobile WiMAX MAC and PHY layer optimization for IPTV

Will Hrudey, Ljiljana Trajković *

Simon Fraser University, Vancouver, British Columbia, Canada

ARTICLE INFO

Article history:
Received 16 January 2010
Received in revised form 28 July 2010
Accepted 5 August 2010

Keywords:
Wireless networks
WiMAX
Video on demand
Internet Protocol TV
Mobile TV
Performance evaluation

ABSTRACT

WiMAX (Worldwide Interoperability for Microwave Access) embodies the IEEE 802.16 family of standards that provision wireless broadband access. With the IEEE 802.16e—2005 mobility amendment, WiMAX promises to address the ever-increasing demand for mobile high speed wireless data in fourth-generation (4G) networks. WiMAX market studies continue to project increased subscriber growth rates and planned carrier trials worldwide. Coupled with these increasing growth rates and higher WiMAX throughput rates, bandwidth intensive video on demand (VoD), Internet Protocol TV (IPTV), and mobile TV services are emerging in the forefront of the mobile arena.

In this paper, we explore and derive optimum system level WiMAX parameters by quantifying network performance using such video-rich services. The video traffic will sufficiently load and stress the network to exploit the potential bandwidth, delay, and mobility limitations. We use the OPNET Modeler to engineer simulation sequences and explore the impact of channel bandwidth, time division duplex (TDD) frame size, advanced antenna systems support, and retransmission schemes using four objective performance metrics while streaming a feature-length movie to a Mobile WiMAX subscriber. The objective of this paper is to provide greater insight into Mobile WiMAX system performance using emerging, load intensive and delay sensitive media streaming services.

1. Introduction

Worldwide Interoperability for Microwave Access (WiMAX) embodies the IEEE 802.16 family of standards that provide fixed and mobile broadband access in the telecommunications landscape. Initially, WiMAX was employed as a last mile broadband access solution, circumventing the significant infrastructure costs of cable and Digital Subscriber Line (DSL) deployments. Recently, Mobile WiMAX has launched WiMAX into fourth-generation (4G) mobile data networks competing for subscribers demanding unprecedented levels of personalized, media-rich services. Consequently, telecommunication carriers are experiencing heightened competitive challenges in an effort to address these evolving subscriber demands. In 2007, there were over one hundred planned carrier trials worldwide. Market researchers are projecting 198% compound annual growth rate in Mobile WiMAX systems [1]. In March 2008, the WiMAX Forum published projections of 133 million subscribers by 2012 [2]. In February 2009, the WiMAX Forum was reporting just under 460 WiMAX fixed and mobile deployments worldwide while over 800 million subscribers were projected by 2010 [3]. Intel has projected that over 1.3 billion people will have access to WiMAX by 2012 [4].

Amidst the rapid WiMAX growth, service providers are deploying innovative applications over broadband core Internet Protocol (IP) networks giving rise to emerging video services such as video on demand (VoD) and real time video streaming. Internet Protocol television (IPTV) technology [5–7] distributes video content over IP networks as both managed and unmanaged services. Managed media services are provided by telecommunication carriers who have provisioned the core IP and access networks thereby retaining control over the quality of service (QoS) to their subscribers [8–10]. Unmanaged media

* Corresponding author. Tel.: +1 778 782 3998; fax: +1 778 782 4951.
E-mail addresses: whrudey@cs.sfu.ca (W. Hrudey), ljilja@cs.sfu.ca (L. Trajković).

0895-7177/$ – see front matter © 2010 Elsevier Ltd. All rights reserved.
doi:10.1016/j.mcm.2010.08.008

services are deployments that have no control over the end-to-end performance between the subscribers and the content services.

To reduce their traffic load requirements, VoD and IPTV services encode uncompressed video content using MPEG-x and H.26x codecs. While these encoded streams are marginally loss-tolerant, their performance is inherently a function of available link bandwidth and delay characteristics. Consequently, various objective performance metrics including packet loss, packet delay, packet jitter, and minimum peak throughput are used to quantify streaming performance over the underlying Mobile WiMAX infrastructure.

In our preliminary analysis [11], we use the OPNET Modeler to simulate bandwidth intensive, delay sensitive, video traffic representative of IPTV and other video-rich applications over WiMAX and ADSL. We explored the technical details and performance of WiMAX broadband access technology and examined whether WiMAX access technology for streaming video applications could provide comparable network performance to ADSL. Their performance is inherently a function of the available bandwidth, buffering, and delay characteristics of the underlying network. We examined four performance factors while streaming two hours of MPEG-4 video content to client subscribers to determine whether WiMAX could deliver access network performance comparable to ADSL for video applications. The simulation results indicated that, while ADSL exhibited superior performance, WiMAX demonstrated promising behavior within the bounds of the defined metrics.

In this paper, we describe an OPNET model to stream the Matrix III feature film (MPEG-4 encoded) from a media service provider located in an Internet Data Center (IDC) to a mobile WiMAX video subscriber travelling across a multi-site system. We significantly extended the preliminary study [11] to include generation and integration of a streaming audio component. We also enhanced the protocol stack to include the real time protocol (RTP) layer. Network topology was redesigned to incorporate WiMAX mobility. We included characterization of WiMAX media access control (MAC) and physical (PHY) layer system parameters. Various MAC and PHY system design parameters were identified, reviewed, and selected on the basis of their potential contribution to maximizing performance and minimizing latencies and loss. The performance metrics were further refined and a system design matrix consisting of four key MAC and PHY parameters was derived. The resulting combinations were individually configured as separate scenarios in the OPNET simulation model. The simulation scenarios were used to observe the impact on the four performance metrics.

This paper is organized as follows. In Section 2, we present a brief overview of the video traffic content. Next, we discuss the performance metrics in Section 3. In Sections 4 and 5, the WiMAX MAC and PHY layers are discussed. Section 6 presents the simulation model while Section 7 details the WiMAX specific design and implementation. Simulation results are reported in Section 8. Finally, we conclude with Section 9.

2. A video content overview

In this section, we give a brief overview of video content that consists of both the audio and the visual information available from media service providers hosting VoD and IPTV services. The content originates from a wide range of sitcoms, newscasts, sporting events, and movies in real time and stored video (VoD) formats. It is structured as a sequence of video frames or images that are transmitted or "streamed" to the subscriber and displayed at a constant frame rate [6]. The video component is coupled (typically separately) with a multi-channel audio component that is also structured as a series of audio frames to collectively comprise the video content. Such content is inherently loss-tolerant yet delay sensitive [12], which implies that video playback on the subscriber stations may tolerate some degree of frame loss. However, delays or variations in inter-frame reception rapidly degrade the overall video playback experience.

The video component of the streaming video content may be characterized by several parameters including video format, pixel color depth, coding scheme, and frame inter-arrival rate. It can also be regarded as a sequence of picture images displayed at a constant rate where each frame contains spatial (within) or temporal (between images) redundancy. Various video coding schemes have been engineered to reduce the raw video size by exploiting this redundancy while balancing quality. These schemes include the International Telecommunications Union (ITU) H.26x and International Standards Organization (ISO) Motion Picture Experts Group (MPEG) codecs.

The audio component of the streaming video content may be viewed as a one or more audio channels encoded into a multi-channel audio stream. Channel configurations range from a single channel to 7.1 configurations consisting of left, center, right, left surround, right surround, left back, right back, and low frequency effects (LFE) channels. However, as one separately encodes additional source channels, the resulting audio stream bandwidth requirements increase. A potential compromise in IP-based video streaming systems is the down-mixing (matrixing) of multi-channel sources into conventional two-channel stereo format (known as stereo surround sound) or to only encode the two main channels. Nonetheless, in addition to the number of channels encoded, various other channel encoding parameters contribute to the overall audio bandwidth requirements. The sample rate and the sample size play a significant role in the stream size. Moreover, the codec compression techniques can be lossy or lossless. Lossy compression techniques remove non-essential audio content while keeping certain frequencies intact whereas lossless techniques ensure faithful reproduction of audio source content while compressing the output.

Video and audio frame inter-arrival rates range from 10 frames to 30 frames per second (fps). This parameter is especially critical because network conditions may impact the frame inter-arrival rates and, if left uncompensated, significantly degrade the playback quality. The necessity of the client station to play back frames at a constant rate amidst variable delays in packet arrivals [12] is illustrated in Fig. 1. Packets carrying video content inherently experience an end-to-end

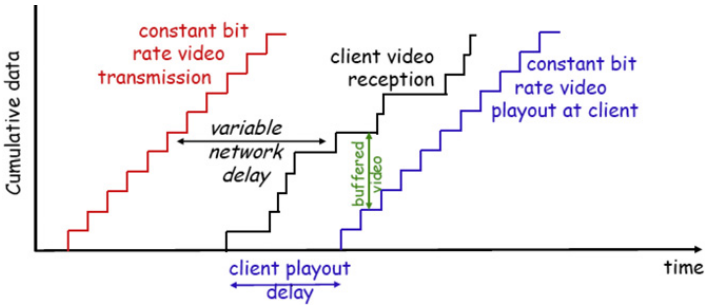

Fig. 1. Buffering required at the video client station [12].

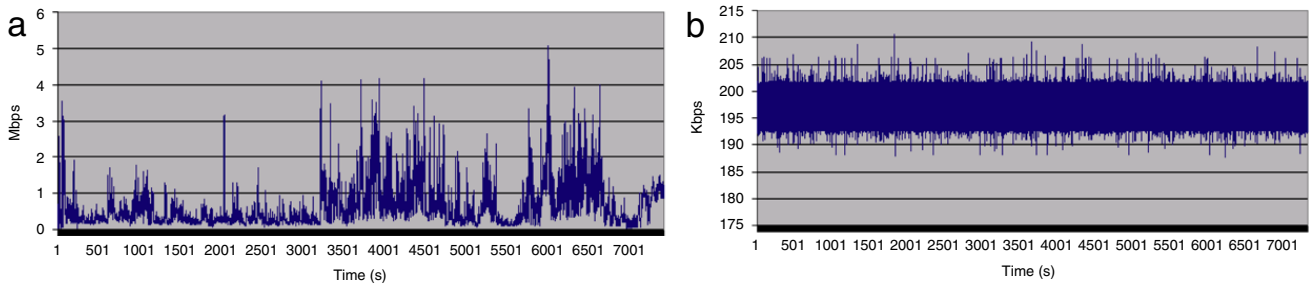

Fig. 2. Throughput requirements: (a) video stream and (b) audio stream.

delay between the sender and the receiver. This delay encompasses the propagation delay and any processing and queuing delays in the intervening routers. Since queuing delays change dynamically and packets may not necessarily traverse the same communication links between the VoD server and the client station, the end-to-end delay will vary. This variation in delay is known as packet delay jitter.

The Matrix III media streams incorporated into this simulation model exhibited video and audio throughput requirements shown in Fig. 2. The video component trace [13,14] was processed into a codec sequence before being imported into the simulation model. The audio component was derived using a custom testbed environment that streamed, captured, and post-processed the multi-channel content of the movie.

3. Performance metrics

In order to assess the performance of video transmission systems, a suite of relevant performance metrics was identified to appropriately benchmark the system. Video on demand (VoD) deployments over best-effort hybrid wireless–wired networks are continually subjected to time varying bandwidth, packet delays, and losses. Since users expect high service quality regardless of the underlying network infrastructure, a number of metrics were collectively used to measure the video content streaming performance to ensure compliance and user quality of experience (QoE).

Performance metrics may be classified as objective and subjective quality measures. Objective measures that observe packet transmissions include packet loss, packet delay, packet jitter, and traffic load throughput rates. Other objective metrics that attempt to quantify video quality perception include the ITU video quality metric (VQM) and peak signal to noise ratio (PSNR), which measure the codec's quality of reconstruction.

The proposed simulation model is trace driven using video and audio traces from the Matrix III movie. However, these traces reflect the individual frame sizes rather than the actual frame data, thereby excluding metrics that rely on actual frame data and playback. As a result, since video playback quality is strongly related to packet loss and end-to-end packet delays [15], the following objective measures, widely used in video content performance analysis [16–21], were employed: packet loss ratio (PLR), packet delay (PD), packet jitter, and minimum throughput. PLR is the number of corrupted, lost, or excessively delayed packets divided by the total number of packets expected at the video client station. PLR can be calculated as [22]

$$PLR = \left(\frac{\text{lost\_packets}}{\text{lost\_packets} + \text{received\_packets}} \right). \tag{1}$$

Packet delay is the average packet transit time between the media server and the video client station. This metric can be calculated as [12]

$$d_{\text{endend}} = Q \left(d_{\text{proc}} + d_{\text{queue}} + d_{\text{trans}} + d_{\text{prop}} \right), \tag{2}$$

where:

Q is the number of network elements between the media server and mobile station;

Table 1
Performance metrics.

Metric	Target
PLR	10^{-3}
Delay (ms)	<400
Jitter (ms)	<50
Throughput (kbps)	221–5311

d_{proc} is the processing delay at a given network element;
d_{queue} is the queuing delay at a given network element;
d_{trans} is the transmission time of a packet on a given communications link between two network elements;
d_{propr} is the propagation delay across a given network link.

Packet jitter or packet delay variation (PDV) is defined as the variability in packet delay within a given media stream at the video client station. This metric can be calculated as

$$j_{\text{pkt}} = t_{\text{actual}} - t_{\text{expected}}, \tag{3}$$

where:

t_{actual} is the actual packet reception time;
t_{expected} is the expected packet reception time.

Throughput is defined as the traffic load that the media stream will impress upon the network. It can be measured in bytes/s (Bps) or bits/s (bps). For constant bit rate (CBR) content, the throughput is constant and it can be calculated as

$$R_{\text{min}} = (\text{frame\_size\_in\_bytes})\ (\text{fps})\ \ (8\ \text{bits/byte}). \tag{4}$$

With variable bit rate encoders, the traffic loading is dynamic in nature and it is a function of the scene complexity and associated audio content. Consequently, variable bit rate (VBR) traffic loads are typically quoted as peak throughput ranges.

The target metric thresholds used in the model and shown in Table 1 reflect the Y.1541 QoS recommendations adopted by IPTV service providers [23]. The throughput threshold was derived from the video and audio trace content.

4. The MAC layer

The WiMAX MAC layer uses the PHY layer to transmit higher level packet traffic in one of three operational modes: point to point (PPP), point to multi-point (PMP), and mesh. In PMP, base stations (BS) service all mobile stations (MS). All MS to MS communications are handled by the BS. In contrast, the mesh mode allows stations to communicate directly. The MAC services and responsibilities are distributed across several sub-layers (shown in Fig. 3) known as the service specific convergence sub-layer (CS) and the common part sub-layer (CPS) [24].

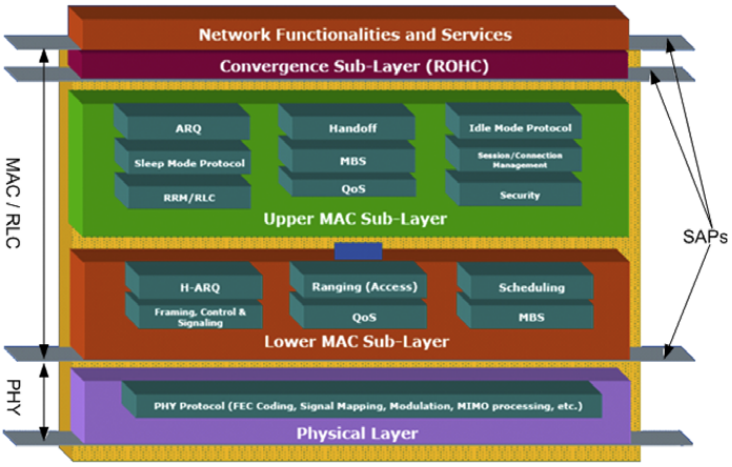

Fig. 3. WiMAX reference model [25].

The QoS scheduling is a major feature in WiMAX systems, which makes it an ideal choice for QoS sensitive applications such as video content streaming. Essentially, radio resources are allocated efficiently and under centralized control within the BS in order to address the service flow's QoS requirements. MAC connections, which are associated with a given service flow, are assigned a QoS scheduling service: one for the DL-MAP and one for the UL-MAP. These scheduling services include

Table 2
MCS and SNR [26,27].

Modulation	Bits/Baud	FEC rate	Spectral efficiency	Receiver SNR (dB)
QPSK	2	1/2	1	5
		3/4	1.5	8
16-QAM	4	1/2	2	10.5
		3/4	3	14
64-QAM	6	1/2	3	16
		2/3	4	18
		3/4	4.5	20
		5/6	5	22

unsolicited grant service (UGS), real time polling system (rtPS), extended real time polling system (ertPS), non-real time polling system (nrtPS), and best effort (BE).

Link adaptation monitors the uplink and downlink quality using the signal to noise ratio (SNR) and adaptively selects the best modulation and coding scheme (MCS) for overcoming time-selective signal fading and maximizing air-link capacity and coverage. Modulation schemes include QPSK, 16-QAM, and 64-QAM, where 64-QAM is optional on the uplink. Channel coding schemes are used to help reduce the SNR requirements by recovering corrupted packets that may have been lost due to burst errors or frequency selecting fading. These schemes generate redundancy bits to accompany information bits when transmitting over a channel. Coding schemes include convolution coding (CC) at various coding rates (1/2, 2/3 and 3/4) as well as convolutional turbo codes (CTC) at various coding rates (1/2, 2/3, 3/4, and 5/6). The coding rate is the ratio of the uncoded block size to the coded block size. For example, a code rate of 1/2 indicates that a block of 12 bytes would be encoded as a block of 24 bytes. Ultimately, the link performance is a trade-off between efficiency and robustness. As channel conditions degrade, the MCS is adaptively downgraded to a more robust, lower order modulation scheme to maintain connection quality and link stability. Similarly, as channel conditions improve, the MCS is adaptively upgraded to a higher, more efficient MCS. The spectral efficiency and minimum receiver SNR for a given MCS are shown in Table 2. Note that SNR values were derived assuming the additive white Gaussian noise (AWGN) environment using tail-biting CC [26].

When forward error correction cannot recover a packet, one of several error handling schemes may be used by WiMAX: automatic repeat request (ARQ), hybrid ARQ (HARQ), combined ARQ/HARQ, or no recovery at all. Both ARQ and HARQ type schemes can be configured per service flow and they may significantly reduce the bit error rate (BER) for a given threshold level. ARQ is strictly a MAC layer function that is used to request lost or corrupted packets using positive and negative acknowledgement. Corrupted packets are discarded at the receiver in this scheme. ARQ has the potential to increase throughput at the trade-off of increased delays from the acknowledgement and retransmission process. In contrast, HARQ, which uses both the MAC and PHY layers, retains the corrupted packets. This allows the receiver to combine the retransmitted packets with the corrupted packets to achieve a higher SNR and coding gain. HARQ can yield very fast retransmissions, as fast as retransmitting in the next frame. The acknowledgements are sent on a dedicated ACK channel and the receiver sends an ACK or NAK in response to each transmission. HARQ has the potential to increase throughput, although not as high as ARQ, without the increased delays introduced by ARQ given the faster detection and retransmission scheme. Combining ARQ and HARQ may potentially yield the best overall performance by delivering higher throughput rates without the higher delays.

5. The PHY layer

The IEEE 802.16 standards have specified PHY access schemes for operation in the 2–11 GHz and 10–66 GHz frequency bands. Consequently, many countries worldwide have allocated one or more frequency bands for WiMAX deployments. However, these allocations are competing with various other commercial and military applications potentially preventing one free universal band worldwide. The key is global harmonization of one or more bands to ensure worldwide roaming of terminal equipment. It has been observed that the success of IEEE 802.11 (also known as WiFi) is credited to the global unification of the 2.4 GHz frequency band. Mobile WiMAX Release-1 profiles cover 5, 7, 8.75, and 10 MHz channel bandwidths in the 2.3, 2.5, 3.3, and 3.5 GHz licensed bands [28]. Moreover, the standards have specified PHY access schemes for operation in the 2–11 GHz and 10–66 GHz frequency bands using conventional single carriers (SCa), orthogonal frequency division multiplexing (OFDM), and orthogonal frequency division multiple access (OFDMA). Various access schemes [24] are shown in Fig. 4. In SCa mode, data from one user are modulated onto a single, conventional wideband RF carrier. With OFDM, which is typically used in fixed WiMAX deployments, data from one user are segmented into smaller chunks and transmitted over one or more orthogonal sub-carriers. Lastly, with OFDMA, which is used in Mobile WiMAX systems, data from multiple users are transmitted over separate sub-channels, which are in turn mapped to one or more orthogonal sub-carriers. Different numbers of sub-carriers can be assigned to different users to support differentiated QoS.

Using OFDM, which takes a higher bit rate input stream and divides it into many lower bit rate parallel streams (and subsequently increased symbol durations), the technical challenges of delay spread, multi-path, and inter-symbol interference (ISI) may be addressed. The increased symbol duration improves the resilience of OFDM to delay spread. Furthermore, a cyclic prefix (CP), which is a repetition of the last samples of the data portion of a block, if longer than the delay

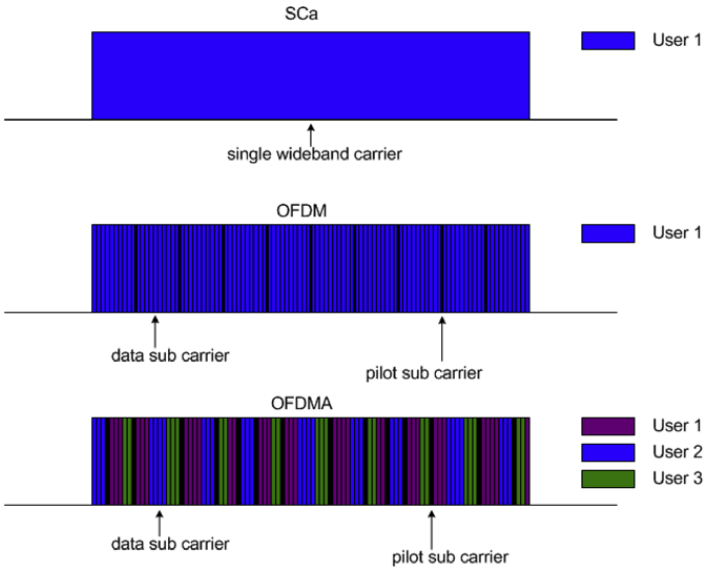

Fig. 4. PHY access schemes [24].

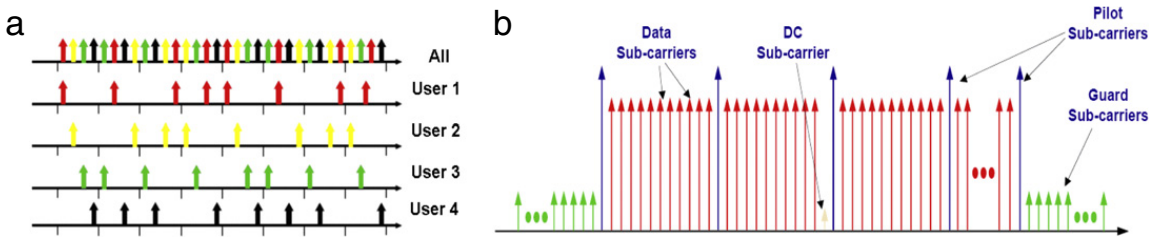

Fig. 5. OFDM: (a) sub-channel allocation and (b) sub-carriers.

spread duration, may eliminate ISI altogether [28]. Each of the parallel, lower bit rate streams is subsequently modulated independently onto one of N sub-carriers (also known as tones). These sub-carriers are closely spaced and overlapped to achieve higher efficiency. Importantly, each sub-carrier's spectrum nulls fall exactly onto the centers of the other sub-carriers, thereby making them orthogonal [29]. Thus, an OFDM signal is comprised of many closely spaced narrowband orthogonal carriers as viewed in Fig. 5(a); since the colored arrows represent data sub-carriers for different users, it is a multi-carrier OFDMA waveform. Ultimately, OFDM is superior for non-line-of-sight (NLOS) applications over conventional single-carrier systems. However, OFDM is sensitive to frequency offsets given the tightly spaced sub-carriers as well as oscillator phase noise. While OFDM could be used for both line of sight (LOS) and NLOS applications, SCa systems should be limited to LOS applications given its inherent inability to satisfactorily perform in multi-path channels.

Channelization in OFDM system is one of the distinguishing factors between OFDM and OFDMA. In OFDMA, sub-carriers are mapped to sub-channels and one or more sub-channels are assigned to a given mobile station. The allocation of sub-carriers to sub-channels is achieved using one of two schemes: distributed and adjacent sub-carrier permutations. The distributed sub-channelization process will utilize full usage of sub-carriers (FUSC) or partial usage of sub-carriers (PUSC). In FUSC, the pilot sub-carriers are allocated first and then the remaining data sub-carriers are divided into sub-channels. However, PUSC pilot and data sub-carriers are partitioned into sub-channels. Downlink sub-frames may use either scheme but uplink sub-frames only use PUSC. The distributed sub-carrier permutation scheme where adjacent sub-carriers are distributed to different sub-channels to increase capacity and frequency diversity while reducing interference through inter-cell interference averaging [24] are shown in Fig. 5(a). Then mobile stations are assigned one or more sub-channels accordingly. Adjacent sub-carrier permutation allocates adjacent sub-carriers to a given sub-channel. This scheme trades off frequency diversity for user diversity. Compared with distributed schemes, which are more resilient to signal fades because the sub-carriers that comprise a given sub-channel are not immediately adjacent to each other, the adjacent scheme is more vulnerable to such propagation effects which makes it inefficient for mobility applications. Nonetheless, sub-channeling concentrates the transmit power into fewer sub-carriers, thereby increasing system gain to extend network coverage, compensate for building penetration losses and reduce power consumption on the mobile stations. Ultimately, this flexibility allows the system designer to trade-off mobility for throughput.

In addition to data sub-carriers used to transport QPSK, 16-QAM, and 64-QAM data symbols, pilot sub-carriers are used for channel estimation purposes by transmitting a known symbol sequence at higher power levels. The DC sub-carrier is typically suppressed to support direction conversion receivers. Guard sub-carriers are suppressed for spectrum shaping purposes and to provide a channel guard. These sub-carriers [24,28,30] are shown in Fig. 5(b). The fast Fourier transform

(FFT) is typically used in OFDM systems to circumvent the need to individually modulate and demodulate many different OFDM sub-carriers. The basic premise is to employ Inverse FFT (IFFT) to generate the waveform and FFT to receive it. IEEE 802.16e−2005 uses bandwidths ranging from 1.25 to 20 MHz [28] with the FFT size scaling accordingly: 128 for 1.25 MHz, 256 for 2.5 MHz, 1024 for 10 MHz, and 2048 for 20 MHz [29]. Consequently, this scheme preserves the fixed sub-carrier spacing for all channel bandwidths and it is otherwise known as scalable OFDMA (SOFDMA).

WiMAX multiplexes uplink and downlink data using one of two duplexing schemes: frequency division duplex (FDD) or time division duplexing (TDD). TDD results in less complex transceiver designs and, subsequently, cheaper implementations and channel reciprocity because the DL and UL frames are sent in the same band [31]. The DL and UL sub-frames (shown in Fig. 6) are separated by a guard time slot called transmit receive transition gap (TTG) [32]. TDD frames are separated by the receive/transmit transition gap (RTG). From a QoS perspective, TDD can dynamically allocate UL and DL bandwidths on the basis of instantaneous loading conditions whereas FDD generally has fixed and equal UL and DL bandwidths. While TDD systems incur the additional guard band, this also allows TDD systems to use advanced antenna techniques.

Multiple-input/multiple-output (MIMO) is a technique where multiple antennas are used at the transmitter and receiver to increase coverage and throughput without increasing bandwidth or transmit power. MIMO achieves this by delivering higher spectral efficiency and link reliability. Fig. 7 shows various antenna configurations and adaptations of MIMO with single and multiple inputs and outputs [33]. There are several types of MIMO that may be employed with WiMAX: beamforming (BF), space–time block code (STBC), and spatial multiplexing (SM). With single-layer BF, the same signal is transmitted on all antennas. However, the antenna phase weights are adjusted to maximize signal strength at the receiver. The increased signal strength is achieved by constructive combining and multi-path fading reduction. With STBC, the same single signal stream is encoded differently, using space–time coding techniques on different antennas to exploit the various received versions of data leading to improved transfer reliability. STBC leverages off independent fading in multiple-antenna systems to create signal diversity and therefore can increase coverage without increasing the peak throughput rates [34]. SM takes the higher rate transmit signal and divides it into lower rate streams where each lower rate stream is transmitted on the same frequency but on different antennas. The receiver can separate these parallel streams if they are received with sufficiently unique spatial signatures [33]. This technique can actually increase peak throughput when channel conditions are good. However, when channel conditions degrade, the packet error rate (PER) may increase, thereby reducing the coverage area. WiMAX supports dynamic switching between these MIMO techniques to maximize coverage and capacity on the basis of channel conditions. This is known as adaptive MIMO switching (AMS) [34]. The OPNET Modeler currently supports STC 2×1 MIMO only.

6. The simulation model

We selected the OPNET Modeler simulation tool [35] because of its widespread adoption in both commercial and military domains. The adopted model topology is comprised of a Mobile WiMAX access network in Vancouver connected to the Internet via a 155.52 Mbps OC-3 PPP link. On the fixed network, VoD/IPTV services are provisioned in an IDC located in Toronto with a 10 Gbps OC-192 backbone connection. The global network topology is shown in Fig. 8. In order to include link propagation delays and PHY behavior across varying distances between the Mobile WiMAX video client and base stations, a global coordinate system was adopted to describe node locations using latitude, longitude, and elevation. The WiMAX gateway router is approximately 3350 km from the IDC, which introduces a propagation delay of approximately 13.3 ms in each direction. The overall concept of a remote IDC furnishing IPTV related services is reasonable given the high throughput rates over the optical links and the small propagation delay in relation to the overall acceptable end-to-end delays for video streaming systems.

The Internet cloud in Fig. 8 was configured with a 0% packet loss and 32.7 ms delay for all packets entering the cloud. These numbers were empirically derived by running a continuous ICMP echo request/echo response test using a 1400 byte maximum transfer unit (MTU) between a LAN-based node in Vancouver and a major backbone router (gw02.wlfdle.phub.net.cable.rogers.com) in Ontario over a 24 h period that covered both peak and non-peak periods on these links. The observed packet loss was 0% with approximately 92 ms round trip times on average, which is equal to approximately 46 ms each way. Moreover, this backbone router exhibited 0% packet loss and 46 ms delays over the previous 24 h interval [36] from the instance when the sample was taken. Since the 46 ms one-way delay reported by the ping tool includes the inherent propagation delay of approximately 13.3 ms, a configured delay of 32.7 ms was adopted because the OPNET Modeler separately calculates and models the propagation delays.

While a typical IDC would have redundant servers, redundant network interfaces and links, network management systems (NMS), storage area networks (SAN), backup power and cooling systems, a simplified topology used in simulations is shown in Fig. 9. A single IBM p690 16 CPU machine serves as the VoD server, which in turn is connected to a gigabit LAN. The network connections between the server and the network elements including the switch and routers are 1 Gbps. The local client "control" machine has been incorporated into the model to serve as the control in this simulation experiment. This station was used extensively in troubleshooting various streaming aspects of the system during the development of the model. In the later stages of development, it served as a best-case reference station for validation of the WiMAX mobile station performance.

The WiMAX access network is shown in Fig. 10. Using a GPS mapping tool [37], a high level map of the Vancouver area was imported into the model by defining map boundaries. The surrounding terrain in this region is generally flat and,

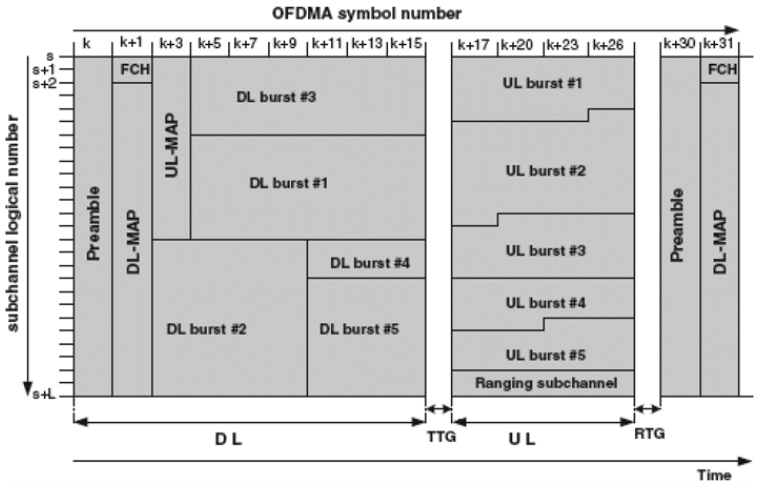

Fig. 6. Single TDD frame [32].

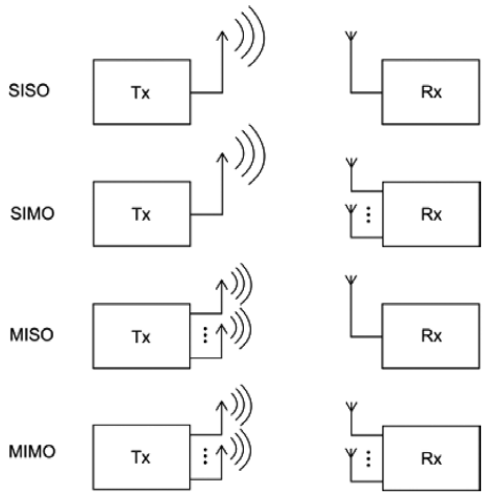

Fig. 7. Antenna configurations [33].

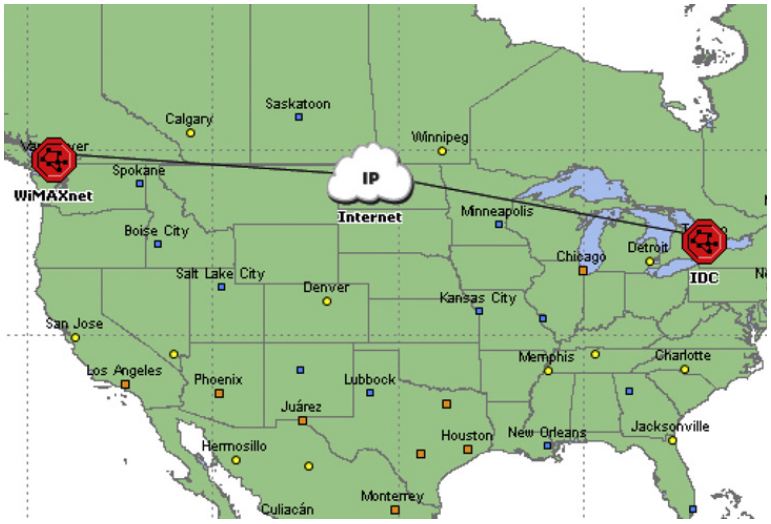

Fig. 8. Global network topology.

therefore, ideal for exploiting simulated coverage and performance testing. The Mobile WiMAX station will travel along a given trajectory at varying distances from site towers to facilitate the WiMAX MAC and PHY layer optimization.

This is a trace driven model utilizing video and audio traces from the Matrix III motion picture movie and, hence, the trace files had to be configured into the model. The trace files are placed into a working directory included in the Modeler's

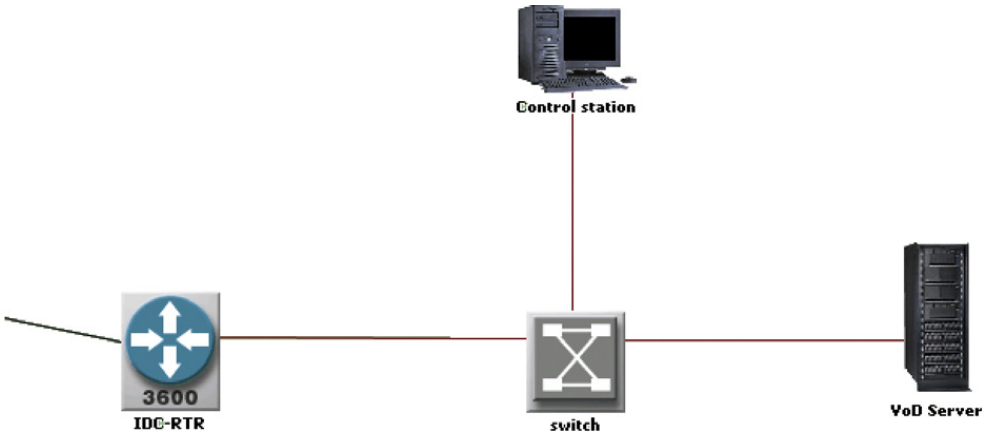

Fig. 9. IDC VoD services network.

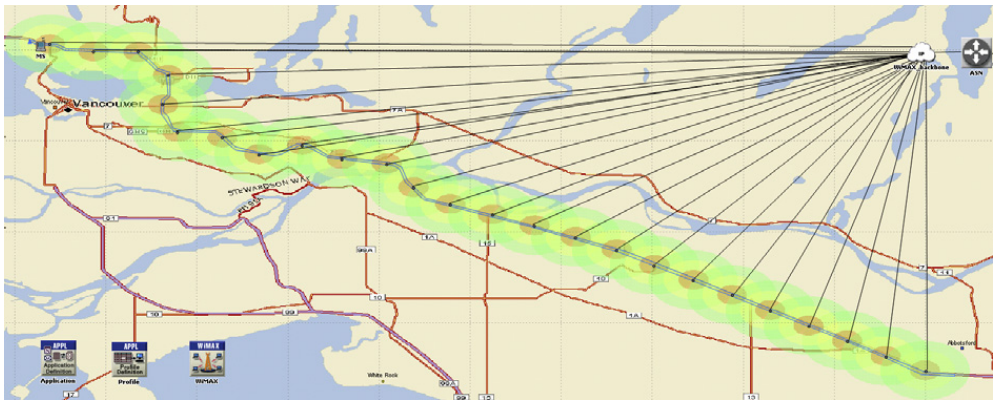

Fig. 10. Mobile WiMAX access network.

model directories path (mod_dir). The profile configuration is configured to simultaneously stream two applications. Two independent instances of the video conferencing application are used to stream the separate and distinct video and audio components of the movie. The key parameters of this configuration are the frame inter-arrival time and frame size. The incoming inter-arrival times are configured to the video and audio frame rates of 25 and 21.6 (derived from audio testbed), respectively. It should be noted that the outgoing inter-arrival time remains set to "none" in order to achieve unidirectional streaming from the VoD server. Furthermore, the frame size parameters are configured to explicitly script the video and audio traces; the.csv extension is not included in the fields. In order for the unidirectional streaming to work, the Modeler still required the outgoing frame sizes to be configured similarly to the incoming frame size configuration.

After the individual content streams were configured to drive the simulation, the profile configuration was explored in detail to ensure that the streams were set up in a suitable yet predictable manner. While the video and audio streams are managed as separate RTP streams [38], the profile was set up to ensure that the "application" streams were launched concurrently rather than serially at the same time offset, for the same overall duration. Both streams were set up to commence streaming 60 s into the simulation. This 60 s interval is important for permitting sufficient time for the routes of the routing information protocol (RIP) to converge across the network. The typical convergence time observed in this model was approximately 30 s. Thereafter, the simulation streamed content for 7380 s (123 min). Given that each content stream is encoded as a separate RTP stream, video and audio content are independently packetized and submitted to the network. Consequently, the two RTP streams may experience different delays, jitter, and loss. The overall simulation time was 7500 s (125 min), which accommodated a 60 s idle period after the end of the movie to allow the network and captured statistics to return to the steady state.

7. The WiMAX configuration

The WiMAX system parameters that were identified and reviewed as candidate parameters that network operators could most practically optimize for streaming video content are:

- duplexing scheme (TDD versus FDD);
- operating frequency (2.3, 2.5, 3.5 GHz);
- channel bandwidth (5, 7, 8.75, 10 MHz);
- TDD DL/UL ratio (3:1, 1.5:1, 1:1);

Table 3
MAC/PHY system design parameter matrix.

Channel bandwidth (MHz)	Frame duration (ms)	Advanced antenna systems	ARQ scheme
5	5	None (SISO)	None
			ARQ/HARQ
		STC 2 × 1 MIMO	None
			ARQ/HARQ
	20	None (SISO)	None
			ARQ/HARQ
		STC 2 × 1 MIMO	None
			ARQ/HARQ
7	5	None (SISO)	None
			ARQ/HARQ
		STC 2 × 1 MIMO	None
			ARQ/HARQ
	20	None (SISO)	None
			ARQ/HARQ
		STC 2 × 1 MIMO	None
			ARQ/HARQ
10	5	None (SISO)	None
			ARQ/HARQ
		STC 2 × 1 MIMO	None
			ARQ/HARQ
	20	None (SISO)	None
			ARQ/HARQ
		STC 2 × 1 MIMO	None
			ARQ/HARQ

- TDD frame size (2–20 ms);
- AAS (SISO, STC 2 × 1 MIMO);
- sectored base stations;
- ARQ, HARQ and ARQ/HARQ;
- base station transmit power;
- QoS schedulers (UGS, rtPS, ertPS, nrtPS, BE);
- AMC versus specific MCS;
- FFT size and sub-carrier spacing;
- network topology considerations that impact path loss and multi-path channel fading.

Four parameters were selected as key parameters for optimizing system performance. While there were other parameters of interest, the selection was limited to four parameters, which yielded 24 different deployment configurations. The matrix described in Table 3 highlights the four chosen system parameters: channel bandwidth, TDD frame duration, DL AAS, and retransmission scheme. Each of these parameters was varied according to potential deployment values for a 3.5 GHz Mobile WiMAX system. As an example, for a 5 MHz channel, 5 ms TDD frames are explored for a SISO configuration with and without retransmissions (ARQ). An example on the other end of the configuration spectrum is a 10 MHz channel using 20 ms TDD frames together with STC 2 × 1 MIMO and combined ARQ/HARQ. The Modeler currently supports AAS techniques on the DL only.

The channel bandwidths currently supported in Mobile WiMAX Release 1 for 3.5 GHz operation were 5, 7, and 10 MHz. The TDD frame durations ranged from 2 to 20 ms and, hence, the matrix exploited performance at the upper and lower boundaries of the frame size. A 5 ms frame duration has a faster response at the trade-off of increased overhead since the overhead is fixed, while the 20 ms has lower overhead in relation to the 5 ms frame at the cost of a slower system response. The advanced antenna systems (AAS) parameter values were limited to the two supported schemes in the OPNET Modeler. A SISO scheme describes a basic station configuration with one transmitter and one receiver; this configuration represents the lower end of achievable system performance. A 2 × 1 MIMO system (known as a MISO system) is also modeled using STC to exploit the independent fading characteristics in a multiple-antenna system configuration to increase coverage. The final parameter was the inclusion or exclusion of a retransmission scheme (ARQ/HARQ) for erroneous frames that cannot be recovered by FEC.

The proposed OFDM design parameters for 5, 7, and 10 MHz channels for 5 and 20 ms frames are described in Table 4. For each channel bandwidth, both time and frequency resources are assigned. The sampling factor n is channel size dependent where channels that are a multiple of 1.75 MHz should use $n = 8/7$ and channels that are multiples of 1.25, 1.5, 2, or 2.75 MHz should use $n = 28/25$ [26,30]. Consequently, the sampling factor is applied to a given channel bandwidth size to determine the sampling frequency (F_s). The respective sample time is determined by taking the inverse of F_s.

The sampling frequency f is then divided by the FFT size (N_{FFT}) to derive the sub-carrier spacing. This concept is the underlying premise in SOFDMA systems, which scale the FFT size to the channel bandwidth in order to maintain the same fixed sub-carrier spacing across different channel sizes. In doing so, this scheme keeps the basic OFDMA symbol resource

Table 4
OFDMA channel design for a 5 and 20 ms frame.

System Parameters		5 ms frame			20 ms frame		
System channel bandwidth in MHz		5	7	10	5	7	10
Sampling factor [n]		1.12	1.14	1.12	1.12	1.14	1.12
Sampling frequency in MHz [Fs]		5.60	8.00	11.20	5.60	8.00	11.20
Sample time (ns)		178.57	125.00	89.29	178.57	125.00	89.29
FFT Size (N_{FFT})		512	1024	1024	512	1024	1024
Sub carrier frequency spacing (kHz)		10.94	7.81	10.94	10.94	7.81	10.94
Useful symbol time (μs) [T_b]		91.43	128.00	91.43	91.43	128.00	91.43
Guard time (μs) [T_g]		11.43	16.00	11.43	11.43	16.00	11.43
OFDMA symbol duration (μs) [T_s]		102.86	144.00	102.86	102.86	144.00	102.86
Frame duration (ms)		5	5	5	20	20	20
Number of OFDMA symbols		48	34	48	194	138	194
DL MAC overhead (symbols)		1	1	1	1	1	1
UL MAC overhead (symbols)		1	1	1	1	1	1
TTG overhead (symbols)		1	1	1	1	1	1
Data symbols		45	31	45	191	135	191
DL/UL ratio		3	3	3	3	3	3
DL data symbols		34	23	34	143	101	143
UL data symbols		11	8	11	47	33	47
DL	Null subcarriers left	46	92	92	46	92	92
	Null subcarriers right	45	91	91	45	91	91
	Data subcarriers	360	720	720	360	720	720
	Pilot subcarriers	60	120	120	60	120	120
	Subchannels	15	30	30	15	30	30
	Data subcarriers / subchannel	24	24	24	24	24	24
	Mode	PUSC	PUSC	PUSC	PUSC	PUSC	PUSC
UL	Null subcarriers left	52	92	92	52	92	92
	Null subcarriers right	51	91	91	51	91	91
	Data subcarriers	272	560	560	272	560	560
	Pilot subcarriers	136	280	280	136	280	280
	Subchannels	17	35	35	17	35	35
	Data subcarriers / subchannel	16	16	16	16	16	16

unit fixed, thereby minimizing the impact on higher layers across different channel sizes [39,40]. Thus, the N_{FFT} for 5, 10, and 20 MHz channels are 512, 1024, and 2048 respectively. The expressions for FFT and IFFT are

$$\text{FFT: } Y(k) = \sum_{n=0}^{N-1} X(n) W_N^{-nk}, \quad k = 0, 1, 2, \ldots, N-1 \tag{5}$$

$$\text{IFFT: } Y(k) = \frac{1}{N} \sum_{n=0}^{N-1} X(n) W_N^{nk}, \quad k = 0, 1, 2, \ldots, N-1. \tag{6}$$

Note, however, that the WiMAX forum [28] proposed that 7 and 8.75 MHz channels still use an N_{FFT} of 1024. The design for the proposed simulation model has followed the WiMAX forum recommendation.

Once the sub-carrier spacing f has been derived, the useful symbol time can be calculated as

$$T_b = \frac{1}{f}. \tag{7}$$

The symbol guard time, T_g, is expressed as

$$T_g = T_b \text{CP}, \tag{8}$$

where the cyclic prefix (CP) is a key parameter in eliminating the inter-symbol interface (ISI) mentioned earlier. The CP is actually a sequence of data from the end of the symbol, which is ultimately repeated at the beginning of the symbol. This effectively creates a sliding time window of T_b, which can vary its position by as much as T_g and still recover the entire symbol without inter-symbol interference [29]. Mobile WiMAX supports CP values of 1/32, 1/16, 1/8, and 1/4 [26]. An example of how the CP guard interval protects the adjacent data periods on the receiver [41] is shown in Fig. 11.

The OFDM symbol duration T_s is expressed as the sum of the useful symbol time and the guard interval:

$$T_s = T_b + T_g. \tag{9}$$

The number of OFDMA symbols within a TDD frame is calculated by dividing the frame duration by the T_s. Since the 5 and 10 MHz channels scaled N_{FFT} proportionally, the two channel sizes utilize the same number of symbols, as shown in Table 4. Furthermore, since the adopted duplexing scheme is TDD, the uplink and downlink share the same channel bandwidth and,

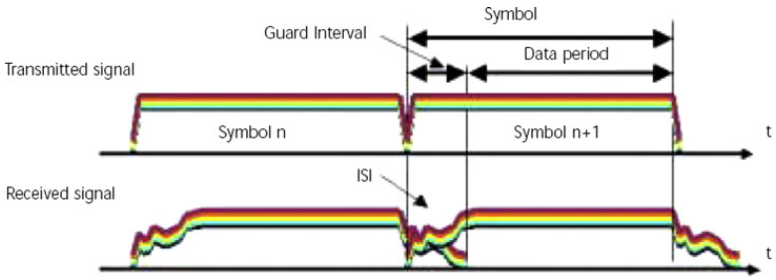

Fig. 11. Inter-symbol interference [41].

ultimately, the same time and frequency resources. Therefore, unlike FDD, TDD should assign a portion of the TDD frame between the DL and the UL, which is described as the DL/UL ratio. In contrast to voice-centric systems, data-centric systems are typically biased to the DL, resulting in an asymmetric allocation of the frame across the DL and UL. While this ratio can be dynamic in practical deployments, the OPNET Modeler requires a fixed number of symbols or percentage of overall symbols. A reasonable and typical DL/UL ratio is 3:1 [24,28,31,34,42] and it is consequently used in this model. For example, if a system configuration has 44 data symbols, then 33 symbols would be allocated to the DL sub-frame and 11 symbols would be allocated to the UL sub-frame.

Lastly, the MAC related overhead associated with the preamble, FCH, DL-MAP, UL-MAP, DCD, UCD, IRI, BRI, ACK-CH, CQICH, TTG, and RTG needs to be accounted for in terms of overhead symbols. While the MAC overhead can vary from frame to frame, for the purposes of modeling and effective throughput calculations, a discrete number of symbols are allocated to DL and UL overhead and the remaining symbols are used as data symbols.

In the frequency resource domain, the fixed spaced sub-carriers across the channel bandwidth are allocated as null, data, and pilot sub-carriers independently for the DL and UL. The IFFT and forward FFT are used to efficiently modulate and demodulate the OFDM sub-carriers so the scaled N_{FFT} size determines the number of sub-carriers for a given channel bandwidth. The UL typically apportions fewer data sub-carriers and more pilot sub-carriers than the DL counterpart to help the BS synchronize with the power-limited MS since pilot tones are transmitted 3 dB higher for channel estimation purposes.

Once the distribution of carriers is complete, the raw and effective PHY and MAC throughputs can be calculated using the number of data sub-carriers, OFDMA symbols per sub-frame, frame duration, and information bits per symbol. The approximate channel capacities as well as the effective throughput rates as a function of the modulation and coding schemes are shown in Table 5. Naturally, the wider the channel bandwidth and/or the higher the MCS, the higher the throughput rates, since wider channels have more data sub-carriers and higher order MCS encode more information bits per symbol. This table is based on the specific channel designs (SISO) shown in Table 4 and, consequently, represents effective rates that factor in MAC and PHY overhead.

For a given channel bandwidth, the data sub-carriers are logically grouped into sub-channels where the uplink groups 16 sub-carriers into a sub-channel while the downlink groups 24 sub-carriers into a sub-channel [28]. Consequently, as the channel bandwidth increases, the number of available sub-channels that can be assigned to mobile stations increases. The number of symbols per sub-carrier is a function of the symbol and frame durations as described previously. On the basis of the DL/UL ratio, the number of symbols per sub-frame is the product of the number of symbols per sub-carrier and the number of symbols per sub-frame. The UL and DL capacities are calculated by dividing the frame duration into the UL and DL symbols per sub-frame. The capacities are measured in millions of symbols per second (Msps) and provide a basis for comparison between channel bandwidths. Finally, the throughput rates for a given channel reflect the product of the channel capacity and the number of information bits per symbol.

In Tables 4 and 5, the TTG, which reflects the sub-frame guard time where the base station switches from transmit to receive and the mobile stations switch from receive to transmit, is assumed to consume one symbol duration. The RTG, which reflects the inter-frame guard time where the base station switches from receive to transmit and the mobile stations switch from transmit to receive, is typically smaller and, therefore, not factored into these approximation tables. Consequently, there is satisfactory agreement between the tables and the BS admission control statistics generated by the OPNET Modeler. In the model design, the configured TTG and RTG values are channel size dependent and they followed the recommendations outlined in the Mobile WiMAX system profiles [43]. Specifically, the derivation of their values is based on a recommended integer multiples of the physical slots (PS):

$$\mathrm{PS} = \frac{4}{F_s}, \tag{10}$$

where F_s is the sampling frequency. The configured values for TTG and RTG for various channel bandwidths are shown in Table 6. As an example, for a 5 MHz channel, TTG is 148 times the PS, which is equivalent to 106 μs.

In order to produce more conservative results, which would represent the lower end of the system performance, a frequency reuse scheme (FRS) value of 1 was adopted in the model design. This implies that all cells operate on the same frequency channel to maximize spectral efficiency. While the potential risk with this scheme is degraded performance observed by mobile stations at the cell edge, the inherent nature of Mobile WiMAX and it sub-channelization characteristics

Table 5
Effective throughput rates for 5 and 20 ms frames.

Frame duration		5 ms								20 ms							
Modulation scheme		QPSK		16-QAM		64-QAM				QPSK		16-QAM		64-QAM			
Bits / symbol		2	2	4	4	6	6	6	6	2	2	4	4	6	6	6	6
Code rate		1/2	3/4	1/2	3/4	1/2	2/3	3/4	5/6	1/2	3/4	1/2	3/4	1/2	2/3	3/4	5/6
Info bits / symbol		1	1.5	2	3	3	4	4.5	5	1	1.5	2	3	3	4	4.5	5
5 MHz	DL subchannels	15	15	15	15	15	15	15	15	15	15	15	15	15	15	15	15
	UL subchannels	17	17	17	17	17	17	17	17	17	17	17	17	17	17	17	17
	DL symbols / subcarrier	34	34	34	34	34	34	34	34	143	143	143	143	143	143	143	143
	UL symbols / subcarrier	11	11	11	11	11	11	11	11	47	47	47	47	47	47	47	47
	DL symbols / subframe	12150	12150	12150	12150	12150	12150	12150	12150	51480	51480	51480	51480	51480	51480	51480	51480
	UL symbols / subframe	3060	3060	3060	3060	3060	3060	3060	3060	12784	12784	12784	12784	12784	12784	12784	12784
	DL subframe capacity (Msps)	2.448	2.448	2.448	2.448	2.448	2.448	2.448	2.448	2.574	2.574	2.574	2.574	2.574	2.574	2.574	2.574
	UL subframe capacity (Msps)	0.598	0.598	0.598	0.598	0.598	0.598	0.598	0.598	0.653	0.653	0.653	0.653	0.653	0.653	0.653	0.653
	Total capacity (Msps)	3.046	3.046	3.046	3.046	3.046	3.046	3.046	3.046	3.227	3.227	3.227	3.227	3.227	3.227	3.227	3.227
	DL throughput (Mbps)	2.448	3.672	4.896	7.344	7.344	9.792	11.016	12.240	2.574	3.861	5.148	7.722	7.722	10.296	11.583	12.870
	UL throughput (Mbps)	0.598	0.898	1.197	1.795	1.795	2.394	2.693	2.992	0.653	0.979	1.306	1.958	1.958	2.611	2.938	3.264
	Total throughput (Mbps)	3.046	4.570	6.093	9.139	9.139	12.186	13.709	15.232	3.227	4.840	6.454	9.680	9.680	12.907	14.521	16.134
7 MHz	DL subchannels	30	30	30	30	30	30	30	30	30	30	30	30	30	30	30	30
	UL subchannels	35	35	35	35	35	35	35	35	35	35	35	35	35	35	35	35
	DL symbols / subcarrier	23	23	23	23	23	23	23	23	101	101	101	101	101	101	101	101
	UL symbols / subcarrier	8	8	8	8	8	8	8	8	33	33	33	33	33	33	33	33
	DL symbols / subframe	16740	16740	16740	16740	16740	16740	16740	16740	72720	72720	72720	72720	72720	72720	72720	72720
	UL symbols / subframe	4340	4340	4340	4340	4340	4340	4340	4340	18480	18480	18480	18480	18480	18480	18480	18480
	DL subframe capacity (Msps)	3.312	3.312	3.312	3.312	3.312	3.312	3.312	3.312	3.636	3.636	3.636	3.636	3.636	3.636	3.636	3.636
	UL subframe capacity (Msps)	0.896	0.896	0.896	0.896	0.896	0.896	0.896	0.896	0.952	0.952	0.952	0.952	0.952	0.952	0.952	0.952
	Total capacity (Msps)	4.208	4.208	4.208	4.208	4.208	4.208	4.208	4.208	4.588	4.588	4.588	4.588	4.588	4.588	4.588	4.588
	DL throughput (Mbps)	3.312	4.968	6.624	9.936	9.936	13.248	14.904	16.560	3.636	5.454	7.272	10.908	10.908	14.544	16.362	18.180
	UL throughput (Mbps)	0.896	1.344	1.792	2.688	2.688	3.584	4.032	4.480	0.952	1.428	1.904	2.856	2.856	3.808	4.284	4.760
	Total throughput (Mbps)	4.208	6.312	8.416	12.624	12.624	16.832	18.936	21.040	4.588	6.882	9.176	13.764	13.764	18.352	20.646	22.940
10 MHz	DL subchannels	30	30	30	30	30	30	30	30	30	30	30	30	30	30	30	30
	UL subchannels	35	35	35	35	35	35	35	35	35	35	35	35	35	35	35	35
	DL symbols / subcarrier	34	34	34	34	34	34	34	34	143	143	143	143	143	143	143	143
	UL symbols / subcarrier	11	11	11	11	11	11	11	11	47	47	47	47	47	47	47	47
	DL symbols / subframe	24300	24300	24300	24300	24300	24300	24300	24300	102960	102960	102960	102960	102960	102960	102960	102960
	UL symbols / subframe	6300	6300	6300	6300	6300	6300	6300	6300	26320	26320	26320	26320	26320	26320	26320	26320
	DL subframe capacity (Msps)	4.896	4.896	4.896	4.896	4.896	4.896	4.896	4.896	5.148	5.148	5.148	5.148	5.148	5.148	5.148	5.148
	UL subframe capacity (Msps)	1.232	1.232	1.232	1.232	1.232	1.232	1.232	1.232	1.344	1.344	1.344	1.344	1.344	1.344	1.344	1.344
	Total capacity (Msps)	6.128	6.128	6.128	6.128	6.128	6.128	6.128	6.128	6.492	6.492	6.492	6.492	6.492	6.492	6.492	6.492
	DL throughput (Mbps)	4.896	7.344	9.792	14.688	14.688	19.584	22.032	24.48	5.148	7.722	10.296	15.444	15.444	20.592	23.166	25.74
	UL throughput (Mbps)	1.232	1.848	2.464	3.696	3.696	4.928	5.544	6.16	1.344	2.016	2.688	4.032	4.032	5.376	6.048	6.72
	Total throughput (Mbps)	6.128	9.192	12.256	18.384	18.384	24.512	27.576	30.64	6.492	9.738	12.984	19.476	19.476	25.968	29.214	32.46

Table 6
TTG and RTG values.

		Channel bandwidths		
		5 MHz	7 MHz	10 MHz
TTG	PS multiple	148 PS	376 PS	296 PS
	(us)	106	188	106
RTG	PS multiple	84 PS	120 PS	168 PS
	(us)	60	60	60

(OFDMA) imply that mobile users' sub-channels reflect a subset of the entire channel bandwidth, thereby minimizing the impact of co-channel interference (CCI) [28]. Such interference may be further reduced by configuring each base station with a different permutation base, which attempts to map different sub-carriers to sub-channels to minimize the overlap between adjacent sites.

The OPNET Modeler assumes that CCI will only occur with sites that use the same PHY profile and permutation zone and that the sub-frame boundaries perfectly align. It consequently then looks at the two packets, namely a valid packet where the signal is locked to the receiver, and the interference packet. Using the pre-computed sub-carrier overlap tables, for every pair of sub-channels it determines the sub-carriers that overlap while observing this permutation base. Essentially, there is a sub-channel list associated with every packet. This interference noise calculation is performed on the mobile's receiver pipeline stage once for every packet, which overlaps its reception with the current packet in time. Ultimately, this scheme will minimize CCI in light to moderate traffic loads where there is sufficient free data sub-carrier capacity to allow neighboring sites to map non-overlapping sub-carriers for a given channel. However, under heavy loads, the MS will have more sub-channels and, consequently, more underlying sub-carriers, thereby increasing the likelihood of overlap between sites regardless of the permutation base.

The overall MAC and PHY system design parameters excluding mobility parameters are shown in Table 7. An operating frequency of 3.5 GHz was selected given that this is one of the promising bands that may achieve worldwide harmonization. The BS transmit power reflects a carrier class Mobile WiMAX solution [44] with 43 dB m output. The MS parameters reflect a 27 dB m Mobile WiMAX transceiver with 5 dBi antenna gain [45]. Typical antenna heights for the base and mobile stations are 32 and 1.5 m respectively [28] and they consequently were adopted in the design. Importantly, initial designs were implemented in Modeler 14.5.A which only supported convolutional coding and, thus, required higher receiver SNR levels

Table 7
Finalized system design parameters.

Parameter	Value
Number of base stations	25
Number of cells	25
Frequency reuse scheme	1
Channel bandwidth (MHz)	Varied according to matrix
Operating frequency (GHz)	3.5
Base station transmit power including PA (W)	20 (43 dB m)
Mobile station transmit power (W)	0.5 (27 dB m)
Base station antenna gain (dBi)	15
Mobile station antenna gain (dBi)	5
Base station antenna height (m)	32
Mobile station antenna height (m)	1.5
TDD frame duration	Varied according to matrix
Number of base station transmitters (MIMO)	Varied according to matrix
Retransmissions	Varied according to matrix
Coding scheme	CTC
Min. power density on base stations (dB m/sub-channel)	−110
TTG 5/7/10 MHz (us)	106/188/106
RTG (us)	60
Permutation base	0.24
Vehicular speeds (km/h)	50

Table 8
MAC/PHY design matrix results.

Channel Bandwidth (MHz)	Frame Duration (ms)	AAS	ARQ scheme	PLR	Delay (ms)	Jitter (ms)	Rank
5	5	none (SISO)	none	3.13E-02	50.9	0.0051	
			ARQ / HARQ	6.88E-04	53.9	0.0330	2
		STC 2x1 MIMO	none	5.69E-03	51.0	0.0055	
			ARQ / HARQ	6.88E-04	52.4	0.0200	1
	20	none (SISO)	none	3.16E-02	59.7	0.0120	
			ARQ / HARQ	7.44E-04	67.0	0.2650	
		STC 2x1 MIMO	none	5.67E-02	59.4	0.0125	
			ARQ / HARQ	7.34E-04	61.5	0.0934	3
7	5	none (SISO)	none	2.64E-02	50.4	0.0030	
			ARQ / HARQ	6.88E-04	52.7	0.0195	2
		STC 2x1 MIMO	none	2.14E-03	50.5	0.0031	
			ARQ / HARQ	6.86E-04	51.3	0.0118	1
	20	none (SISO)	none	2.67E-02	57.9	0.0100	
			ARQ / HARQ	7.36E-04	64.9	0.1750	
		STC 2x1 MIMO	none	2.15E-03	57.9	0.0090	
			ARQ / HARQ	7.23E-04	59.2	0.0480	3
10	5	none (SISO)	none	4.08E-02	49.9	0.0014	
			ARQ / HARQ	6.89E-04	52.7	0.0210	2
		STC 2x1 MIMO	none	7.68E-03	49.8	0.0014	
			ARQ / HARQ	**6.82E-04**	**50.9**	**0.0112**	1
	20	none (SISO)	none	4.19E-02	57.7	0.0106	
			ARQ / HARQ	7.46E-04	68.1	0.2580	
		STC 2x1 MIMO	none	8.07E-03	57.7	0.0095	
			ARQ / HARQ	7.28E-04	60.2	0.0770	3

for a link operating in the error free region. However, given the initial simulated performance results with base station spacing of 3 km, CTC yielded better performance given the degraded SNR levels at the cell edge. Additionally, numerous scenarios reported a DES log warning entry relating to the power correction issued from the serving BS that would put the MS transmit power beyond its configured 27 dB m limit. Consequently, initial efforts explored the several power density ranges (dB m/sub-channel) to increase the likelihood of the MS connecting to a given BS. Ultimately, the default density of −110 dB m/sub-channel was retained in this model.

8. Simulation results

The 24 scenarios were simulated and the results were collected and are summarized in Table 8. The PLR, end-to-end (E2E) packet delays, and packet jitter are presented for each scenario. The red and orange highlighted rows indicate the poorest and best-performing scenarios for a given channel bandwidth, respectively. The yellow and green highlighted rows indicate second-best-performing and third-best-performing scenarios for a given channel bandwidth. Moreover, the rightmost column of the table provides a numerical ranking within the channel where "1" is the best. The overall best-performing scenario across all bandwidths is highlighted with a blue circle: 10 MHz channel using 5 ms frame duration with MIMO and retransmissions.

As the PLR increases, the E2E delay and jitter increase as well, as shown in Table 8. Moreover, scenarios that did not use AAS and retransmissions typically exhibited much higher loss rates. Retransmissions using combined ARQ/HARQ made very significant improvements in SISO configurations. Additionally, scenario configurations that used 20 ms frame durations

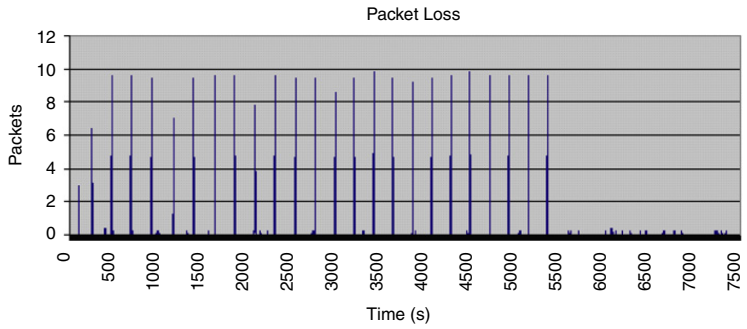

Fig. 12. Packet loss for the top performing configuration.

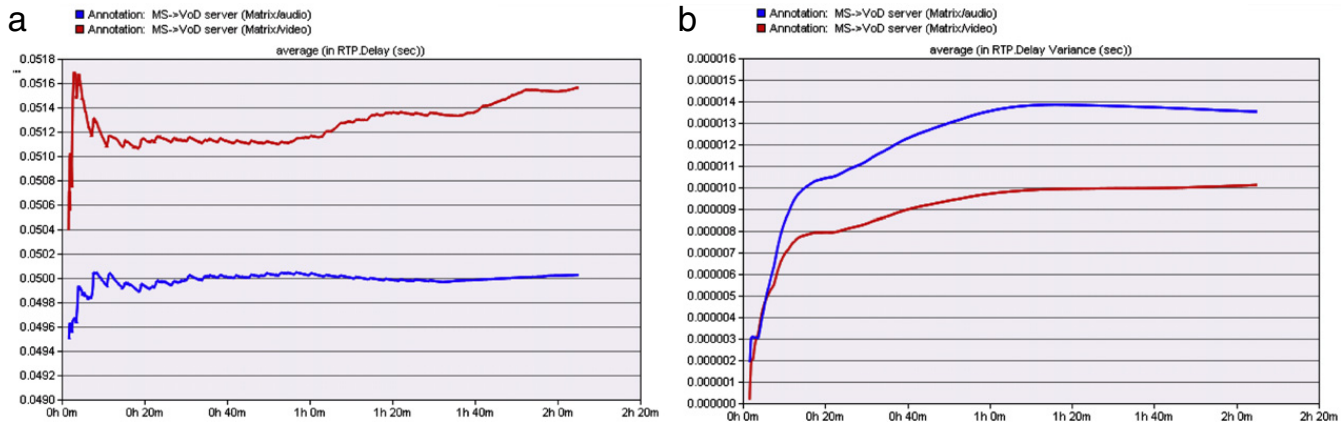

Fig. 13. MS statistics: (a) packet delay and (b) packet jitter.

typically exhibited slightly higher loss rates and delays along with significantly higher packet jitter. Overall, 5 ms frame configurations using MIMO and retransmissions yielded superior results. The highlighted top performing 10 MHz channel configuration delivered comparable loss rates to the 7 and 5 MHz equivalent configurations while yielding lower delay and jitter.

The top performing configuration exhibited the packet loss shown in Fig. 12, which primarily occurred as the MS switched sites. In fact, the MS is disconnected from the serving site and then initiates ranging operations with the next site at which point the packet loss peaks accordingly. This observed model behavior is less than ideal and may be minimized by further refinements of the topology, scanning profiles, and handover parameters. Moreover, once the MS arrives at its destination, it continues to stream video content for the remaining 30 min of the movie. During this period, packet loss is minimal. Video and audio delays are shown in Fig. 13(a) as separate curves where the video delays were slightly higher (3%) than the audio delays. Conversely, the audio packet jitter is slightly higher (within 4 μs) than the video packet jitter as shown in Fig. 13(b).

The last 30 min of the movie were streamed from a single BS and, hence, the site capacity statistics were also reviewed. The DL capacity for a 10 MHz channel using 5 ms frame duration was calculated to be 4.896 Msps, as shown in Table 5. It corresponds to the simulated capacity shown in Fig. 14. During this interval, the DL capacity drops to 4 Msps, thereby indicating that 1 Msps is consumed by the load. At 5 information bits per symbol (64-QAM 5/6), this translates to approximately 5 Mbps, which reflects the peak throughput rates of the video load.

The impact of various overheads and parameters on the capacity of IEEE 802.16e Mobile WiMAX networks carrying mobile TV, VoIP, and data applications has been analyzed using analytical methods [46]. The study has shown that proper use of overhead reducing mechanisms and proper scheduling may significantly improve network performance.

9. Concluding remarks

This developed simulation model delivers positive and insightful results for Mobile WiMAX access link performance under a heavy load representative of IPTV. The MAC and PHY layer design explored the aspects of multi-carrier modulation schemes using SOFDMA including capacity calculations, sub-carrier allocations and permutations, and various modulation and coding schemes and their impact on available throughput rates. The derived MAC and PHY simulation configurations were engineered to reflect realistic and practical Mobile WiMAX deployments.

Fifty per cent of the configuration scenarios achieved performance levels within performance metric thresholds. The 10 MHz channel configuration using 5 ms TDD frame duration with STC 2 $\times$ 1 MIMO and retransmissions achieved the best results. While simulations do not guarantee real world equivalence, these results are encouraging for mobile video transmission systems and reveal that Mobile WiMAX is a formidable player in fourth-generation networks. The simulation

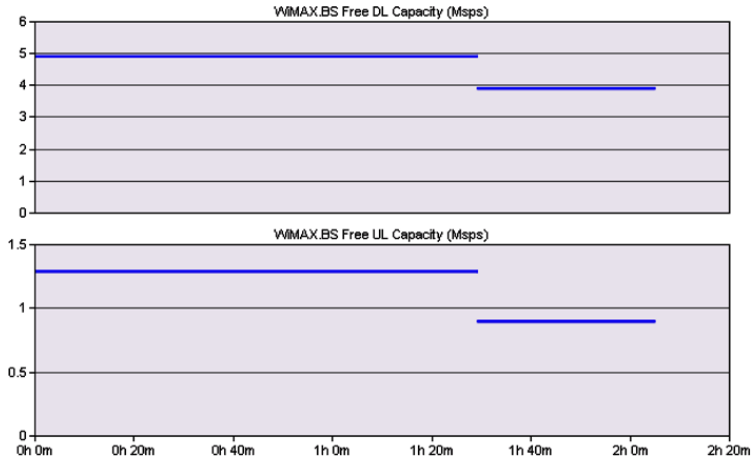

Fig. 14. Final BS downlink and uplink capacities.

results indicate that Mobile WiMAX can deliver sufficient bandwidth while ensuring that E2E packet delays and jitter meet the stringent requirements of video content streaming. Moreover, next generation WiMAX (IEEE 802.16 m) and long term evolution technologies touting even higher spectral efficiencies will pave the way for even richer and higher quality video services such as HDTV.

References

[1] West Technology Research Solutions, Telecom Application Report 2008. Available: http://www.researchandmarkets.com/reports/c81415 [Online].
[2] WiMAX forum. Available: http://www.wimaxforum.org/news/pr [Online].
[3] WiMAX forum press release. Available: http://www.wimaxforum.org/node/644 [Online].
[4] Untethered Publishing Ltd., WiMAX Subscriber Growth. Available: http://www.wimaxday.net/site/wimax-subscriber-growth [Online].
[5] F. Retnasothie, M. Ozdemir, T. Yucek, H. Celebi, J. Zhang, R. Muththaiah, Wireless IPTV over WiMAX: challenges and applications, in: Proc. IEEE WAMICON 2006, Clearwater, FL, December 2006, pp. 1–5.
[6] I. Uilecan, C. Zhou, G. Atkin, Framework for delivering IPTV services over WiMAX wireless networks, in: Proc. IEEE EIT 2007, Chicago, IL, May 2007, pp. 470–475.
[7] J. She, F. Hou, P. Ho, L. Xie, IPTV over WiMAX key success factors, challenges, and solutions, IEEE Communications Magazine 45 (8) (2007) 87–93.
[8] Voice of network convergence, Nortel Names Telus as First IPTV Customer. Available: http://www.von.com/articles/ims-soa/69h1211453923014.html [Online].
[9] MatrixStream technologies, Complete IPTV ASP solution. Available: http://www.matrixstream.com/IPTV_H.264_ASP_solution.php [Online].
[10] Lightwave, Sasktel launches HDTV-based IPTV services. Available: http://lw.pennnet.com/Articles/Article_Display.cfm?Section=ARTCL\&SubSection=Display\&PUBLICATION_ID=13\&ARTICLE_ID=274947 [Online].
[11] W. Hrudey, Lj. Trajkovic, Streaming video content over IEEE 802.16/WiMAX broadband access, OPNETWORK 2008, Washington, DC, August 2008.
[12] J. Kurose, K. Ross, Computer Networking: A Top-Down Approach, 4th ed., Pearson, Addison-Wesley, Boston, MA, 2008, p. 590, p. 612, and p. 624.
[13] G. Auwera, P. David, M. Reisslein, Traffic characteristics of H.264/AVC variable bit rate video, March 2008. Available: http://trace.eas.asu.edu/h264/index.html [Online].
[14] G. Auwera, P. David, M. Reisslein, Traffic and quality characterization of single-layer video streams encoded with the H.264/MPEG-4 advanced video coding standard and scalable video coding extension, March 2008. Available: http://trace.eas.asu.edu/h264/index.html [Online].
[15] V. Vassiliou, P. Antoniou, I. Giannakou, A. Pitsillides, Requirements for the transmission of streaming video in mobile wireless networks, in: Proc. ICANN 2006, September 2006, pp. 528–537.
[16] O. Issa, J. Gregoire, Y. Belala, J. Wong, M. Bage, 3G video uploading applications: performance and improvements, IEEE Multimedia 15 (4) (2008) 58–67.
[17] M. Narbutt, M. Davis, An assessment of the audio codec performance in voice over WLAN (VoWLAN) systems, in: Proc. MobiQuitious 2005, San Diego, CA, July 2005, pp. 461–467.
[18] D. Wu, Y. Hou, W. Zhu, Y. Zhang, H. Chao, MPEG-4 compressed video over the Internet, in: Proc ISCAS 1999, Orlando, Florida, June 1999, pp. 327–331.
[19] P. Calyam, C. Lee, Characterizing voice and video traffic behavior over the Internet. Available: www.osc.edu/research/networking/PDFs/vvoip_iscis05.pdf [Online].
[20] G. Lazar, T. Blaga, V. Dobrota, Framework for IPTV QoS, in: Proc. ELMAR 2008, Zadar, Croatia, September 2008, pp. 161–164.
[21] Y. Chen, H. Yeh, An adaptive polling scheme supporting audio/video streaming in wireless LANs, in: Proc. FTDCS 2008, Kunming, China, October 2008, pp. 16–22.
[22] O. Almomani, S. Hassan, S. Nor, Effects of packet size on FEC performance, in: Proc. NetApps2008, Malaysia, November 2008, pp. 1–4.
[23] IETF, Y.1541 QoS model for networks using Y.1541 QoS classes draft. Available: http://tools.ietf.org/html/draft-ietf-nsis-y1541-qosm-07 [Online].
[24] R. Golshan, Fixed and mobile WiMAX overview. Available: www.fujitsu.com/downloads/MICRO/fma/pdf/esc_wimax06.pdf [Online].
[25] S. Ahmadi, Introduction to mobile WiMAX radio access technology—PHY and MAC architecture. Available:http://www.mat.ucsb.edu/~ggroup/ahmadiUCSB_slides_Dec7.pdf.
[26] IEEE Std. 802.16e—2005: part 16: air interface for fixed and mobile broadband wireless access systems. Available:http://ieee802.org/16/pubs/80216e.html [Online].
[27] IEEE C802.16maint-05/112r8. Available: http://www.ieee802.org/16/maint/contrib/C80216maint-05_112r8.pdf [Online].
[28] WiMAX forum, Mobile WiMAX—part I: a technical overview and performance evaluation. Available: http://www.wimaxforum.org/technology/downloads/Mobile_WiMAX_Part1_Overview_and_Performance.pdf [Online].
[29] SR Telecom Inc., WiMAX technology LOS and NLOS environments. Available: www.srtelecom.com/uploads/File/whitepapers/WiMAX-LOS-and-NLOS-Technology.pdf [Online].
[30] J. Andrews, A. Ghosh, R. Muhamed, The Fundamentals of WiMAX: Understanding Broadband Wireless Networking, 1st ed., Prentice Hall, Upper Saddle River, NJ, 2007.
[31] J. Eira, A. Rodrigues, Analysis of WiMAX data rate performance. Available: http://whitepapers.silicon.com/0,39024759,60579485p,00.htm [Online].
[32] A. Xhafa, S. Kangude, X. Lu, MAC performance of IEEE 802.16e, in: Proc. Vehicular Technology Conference 2005, Stockholm, Sweden, 2005, pp. 685–689.
[33] Wikipedia, MIMO. Available: http://en.wikipedia.org/wiki/Multiple-input_and_multiple-output [Online].

[34] WiMAX forum, Mobile WiMAX—part II: a comparative analysis. Available: http://www.wimaxforum.org/technology/downloads/Mobile_WiMAX_Part2_Comparative_Analysis.pdf [Online].
[35] OPNET Modeler software. Available: http://www.opnet.com/products/modeler/home.html [Online].
[36] Internet traffic report. Available: http://www.internettrafficreport.com/history/249.htm [Online].
[37] Delorme StreetAtlas 2007. Available: http://www.delorme.com [Online].
[38] F. Fitzek, M. Zorzi, P. Seeling, M. Reisslein, Video and audio trace files of pre-encoded video content for network performance measurements (2004), in: Proc. IEEE CCNC 2004, Las Vegas, NV, January 2004, pp. 245–250.
[39] M. Tran, G. Zaggoulos, A. Nix, A. Doufexi, Mobile WiMAX: performance analysis and comparison with experimental results, in: Proc. IEEE Vehicular Technology Conference 2008, Singapore, September 2008, pp. 1–5.
[40] M. Tran, A. Doufexi, A. Nix, Mobile WiMAX MIMO performance analysis: downlink and uplink, in: Proc. IEEE PIMR 2008, Cannes, France, September 2008, pp. 1–5.
[41] Alvarion, Wireless connectivity. Available: http://kambing.ui.edu/onnopurbo/library/library-ref-eng/ref-eng-3/physical/wimax/WP_OFDM.pdf [Online].
[42] WiMAX forum, Mobile WiMAX: a performance and comparative summary. Available:http://www.wimaxforum.org/technology/downloads/Mobile_WiMAX_Performance_and_Comparative_Summary.pdf [Online].
[43] WiMAX forum, Mobile system profile 1.0 revision 1.4.0. Available: www.wimaxforum.org [Online].
[44] Redline Communications, RedMAX 4C SC-1000 mobile WiMAX base station. Available: http://www.redlinecommunications.com/news/resourcecenter/productinfo/SC1000_Mar%205%202009.pdf [Online].
[45] Redline Communications, RedMAX 4C RPM. Available: http://www.redlinecommunications.com/news/resourcecenter/productinfo/RPM.pdf [Online].
[46] C. So-In, R. Jain, A.-K. Tamimi, Capacity evaluation for IEEE 802.16eMobileWiMAX, Journal of Computer Systems, Networks, and Communications, 2010, Article ID 279807, Hindawi Publishing Co., doi:10.1155/2010/279807.